

C–N–P interactions control climate driven changes in regional patterns of C storage on the North Slope of Alaska

Yueyang Jiang · Adrian V. Rocha · Edward B. Rastetter · Gaius R. Shaver ·
Umakant Mishra · Qianlai Zhuang · Bonnie L. Kwiatkowski

Received: 31 March 2015 / Accepted: 19 August 2015
© Springer Science+Business Media Dordrecht 2015

Abstract

Context As climate warms, changes in the carbon (C) balance of arctic tundra will play an important role in the global C balance. The C balance of tundra is tightly coupled to the nitrogen (N) and phosphorus (P) cycles because soil organic matter is the principal source of plant-available nutrients and determines the spatial variation of vegetation biomass across the North Slope of Alaska. Warming will accelerate these nutrient cycles, which should stimulate plant growth.

Objectives and methods We applied the multiple element limitation model to investigate the spatial distribution of soil organic matter and vegetation on the North Slope of Alaska and examine the effects of changes in N and P cycles on tundra C budgets under climate warming.

Results The spatial variation of vegetation biomass on the North Slope is mainly determined by nutrient mineralization, rather than air temperature. Our simulations show substantial increases in N and P mineralization with climate warming and consequent increases in nutrient availability to plants. There are distinctly different changes in N versus P cycles in response to warming. N is lost from the region because the warming-induced increase in N mineralization is in excess of plant uptake. However, P is more tightly cycled than N and the small loss of P under warming can be compensated by entrainment of recently weathered P into the ecosystem cycle. The increase in nutrient availability results in larger C gains in

Special issue: Macrosystems ecology: Novel methods and new understanding of multi-scale patterns and processes.

Guest Editors: S. Fei, Q. Guo, and K. Potter.

Electronic supplementary material The online version of this article (doi:[10.1007/s10980-015-0266-5](https://doi.org/10.1007/s10980-015-0266-5)) contains supplementary material, which is available to authorized users.

Y. Jiang (✉)
Department of Forest Ecosystems and Society, Oregon
State University, Corvallis, OR 97331, USA
e-mail: yueyang.jiang@oregonstate.edu

U. Mishra
Environmental Science Division, Argonne National
Laboratory, 9700 South Cass Ave, Bldg 240, Argonne,
IL 60439, USA

Y. Jiang · E. B. Rastetter · G. R. Shaver ·
B. L. Kwiatkowski
The Ecosystems Center, Marine Biological Laboratory, 7
MBL Street, Woods Hole, MA 02543, USA

Q. Zhuang
Department of Earth, Atmospheric, and Planetary
Sciences, Purdue University, West Lafayette, IN 47907,
USA

A. V. Rocha
Department of Biology, University of Notre Dame,
Notre Dame, IN 46556, USA

vegetation than C losses from soils and hence a net accumulation of C in the ecosystems.

Conclusions The ongoing climate warming in Arctic enhances mineralization and leads to a net transfer of nutrient from soil organic matter to vegetation, thereby stimulating tundra plant growth and increased C sequestration in the tundra ecosystems. The C balance of the region is predominantly controlled by the internal nutrient cycles, and the external nutrient supply only exerts a minor effect on C budget.

Keywords Climate warming · Nutrient budget · C balance · Nutrient limitation · C-nutrient interaction

Introduction

As global climate warms, changes in the carbon (C) balance of arctic tundra ecosystems will play an important role in the global C balance (Sitch et al. 2007; McGuire et al. 2012). Lower air temperature, short growing seasons, shallow soil active layers, and nutrient availability have historically limited tundra vegetation productivity (Callaghan et al. 2005; Hobbie et al. 2005; Shaver and Jonasson 2001; Shaver et al. 2001). Cold soil temperatures also limit soil C turnover (Hobbie et al. 2000; Shaver et al. 2006), and arctic soils contain twice the amount of C that is currently in the atmosphere, despite low plant productivity. Climate warming is more pronounced in the arctic than any other region on the planet (Hinzman et al. 2005; Hansen et al. 2007; IPCC 2007), and is expected to have impacts on the arctic C balance. Warming has increased both tundra productivity (e.g., Stow et al. 2004; Goetz et al. 2005; Zhang et al. 2008) and ecosystem respiration over the past several decades (McGuire et al. 2012; Belshe et al. 2013). The impact of climate warming on arctic tundra C balance will depend on whether respiration increases will offset or cancel arctic plant productivity increases (Friedlingstein et al. 2006; Sitch et al. 2007).

In arctic tundra ecosystems, primary productivity is strongly limited by the supply of soil-available nitrogen (N) and/or phosphorus (P). External N and P inputs by deposition, fixation, and weathering are only about 1 % of the internal recycling of N and P by mineralization of soil organic matter (Giblin et al. 1994; Gough et al. 2002, 2012; Hobbie et al. 2005; Hobbie et al. 2006; Shaver and Chapin 1980). Long-term fertilization with N and P

increases arctic tundra above-ground net primary production by ~ 70 % (Mack et al. 2004). Thus, stimulation of soil N and P mineralization under a warming climate may alleviate nutrient limitation on plant growth, and increase ecosystem carbon storage. However, the response of coupled C, N, and P cycles to warming are poorly understood, despite their importance in determining future vegetation productivity and C sequestration in the arctic.

Field observations and experiments have been conducted to analyze the long-term impacts of warming on C balance in the arctic tundra (Oechel et al. 2000; Sistla et al. 2013). However, up-scaling the C budget based on limited field data is insufficient to depict the spatial variation in C budgets over a large geographic area (Lorant et al. 2011), because of the spatial heterogeneity in local weather conditions, vegetation, and soils across the landscape (Hobbie et al. 2002). Model simulations with appropriate calibration and spatially-explicit drivers provide a rigorous way to account for this spatial heterogeneity. This study builds on recent studies by Pearce et al. (2015) and Jiang et al. (2015), which simulate C, N and P interactions in moist acidic tussock tundra and its short- and long-term responses to fire and thermokarst disturbances. We conducted simulations using the Multiple Element Limitation (MEL) model (Rastetter et al. 2013; Pearce et al. 2015; Jiang et al. 2015) to scale up the N and P cycles and their interactions with the C cycle to a large, heterogeneous region, the North Slope of Alaska (Fig. 1a; $\sim 1.7 \times 10^5$ km²), for the period 1901–2100. We chose to perform these model runs for the North Slope region because MEL was parameterized with ecological data from long-term experiments on the North Slope of Alaska and because of the availability of historical and future climate and soil carbon datasets for this region. Our study is aimed at providing insights on C-nutrient interactions and their responses to warming at the scale of the entire North Slope region.

Methodology

Model

We applied the MEL model (version IV; Rastetter et al. 2013) to simulate the C, N, and P interactions in tundra ecosystems for the North Slope of Alaska (Pearce et al. 2015; Jiang et al. 2015). The MEL model

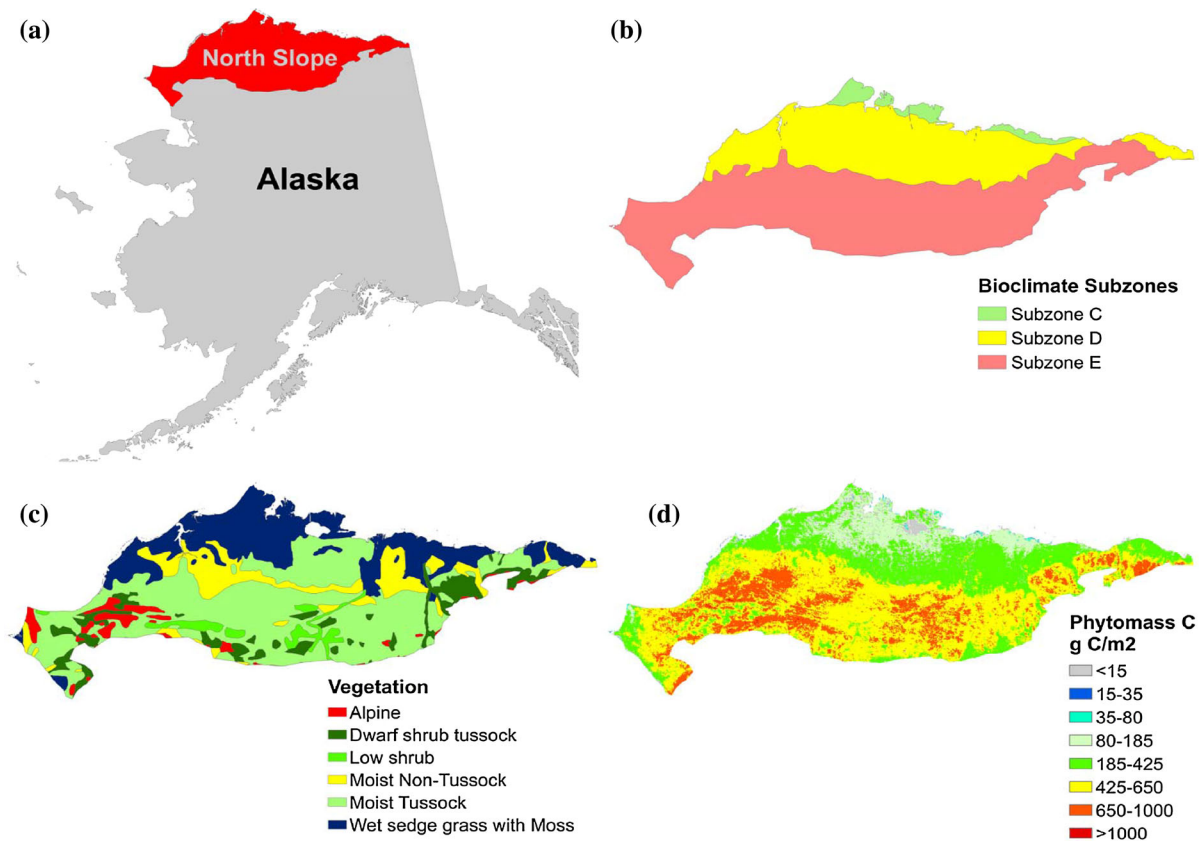


Fig. 1 Location of study area, and its bioclimate subzone, vegetation cover and phytomass C distribution. The bioclimate subzone map, vegetation cover map and phytomass C map are derived from the Toolik-Arctic Geobotanical Atlas (<http://www.arcticatlas.org/>)

simulates the redistribution of plant “uptake effort” to optimize the relative acquisition of resources (Rastetter et al. 1997; Rastetter 2011). The “uptake effort” represents an aggregate of all plant assets (e.g., biomass, enzymes, carbohydrate) allocated toward the acquisition of resources. The allocation of effort is determined by the current requirements for, and the current uptake rates of a specific resource (Rastetter et al. 2013). The requirement is the sum of metabolic consumption and loss in tissue turnover multiplied by a factor to compensate for deviations of the element ratios in the biomass from an optimum.

In the MEL model, vegetation is allometrically partitioned into woody and active biomass, and the latter is further allocated to leaves and fine roots depending on the relative limitation by canopy versus soil resources (Rastetter et al. 2013). Detritus is divided into Phase I and II soil organic matter (SOM; as defined by Melillo et al. 1989), and debris. Phase I SOM represents fallen litter plus younger, more labile

SOM that both mineralizes and immobilizes nutrients, while Phase II SOM only mineralizes nutrients and has a slower turnover rate. Phase I material converts to Phase II material at a rate that is close to 20 % of the C litter flux at steady state (Melillo et al. 1989). Debris represents standing dead leaves and twigs plus any woody litter and is slowly converted to Phase I SOM before it begins to decompose (Hyvönen and Ågren 2001). The MEL model does not simulate the depth of SOM explicitly or SOM in permafrost, but instead predicts total SOM in the annually thawed active layer (above the permafrost table).

The C, N and P balances are linked through vegetation and microbial processes. C enters the ecosystem through photosynthesis, about half of which is respired by the vegetation, the remainder then cycles to soil via litter fall, and eventually is lost from the ecosystem via heterotrophic respiration and loss in dissolved organic matter. N enters as NH_4^+ and NO_3^- via deposition, dissolved organic N (DON), and

non-symbiotic N-fixation. The annual NH_4^+ and NO_3^- deposition rates related to precipitation amount are estimated using year 2000 field-based measurements by Shaver and Laundre (2006). P enters the ecosystem through deposition of PO_4^{3-} or the weathering of primary and secondary P minerals (Rastetter et al. 2013). NH_4^+ and PO_4^{3-} are mineralized from both Phase I and Phase II SOM. Using a Langmuir isotherm (Weatherley and Miladinovic 2004), NH_4^+ , PO_4^{3-} , and DON are partitioned between adsorbed and dissolved fractions and only the latter determines the rates of leaching, nitrification, and uptake by plants and microbes. Nitrate is assumed to completely dissolve in soil water, ready for leaching, and uptake by plants and microbes.

Climate forcing data

The MEL model is driven by daily maximum and minimum air temperature, atmospheric CO_2 concentration, precipitation, and solar radiation. For the period 1901–2009, we obtained the CRU (Climatic Research Unit, TS 3.1; Harris et al. 2014) monthly data (incoming shortwave radiation, air temperature and precipitation) at 1×1 km spatial resolution from the Scenarios Network for Alaska Planning (SNAP 2013). The annual global atmospheric CO_2 concentration was derived from Mauna Loa station (NOAA/ESRL, www.esrl.noaa.gov/gmd/ccgg/trends/). For the period 2010–2100, we used two sets of climate data, a high emission scenario (MPI ECHAM5 SRESA2) and a low emission scenario (MPI ECHAM5 SRESB1). We derived the corresponding A2 and B1 CO_2 concentration from each of the corresponding IPCC SRES scenarios (IPCC 2007). The B1 scenario represents a 163 ppm increase in atmospheric CO_2 concentration from 2009 to 2100, and the A2 scenario, a 468 ppm increase (Fig. 2). Air temperature generally decreased from south to north. The average annual air temperature of the whole North Slope increases from -9.6 °C in 2000 to -6.0 °C in 2100 under the B1 scenario, and to -2.3 °C in years 2090–2099 under the A2 scenario. There was no clear long-term trend in the radiation data. There was no long-term trend in the mean annual radiation, but the year-to-year variability is substantially larger during the 21st century than the 20th century. The mean annual total precipitation of the whole North Slope has large annual variability over the 200 years [varied between (200,

500) mm], and increases ~ 60 mm under B1 and ~ 110 mm under A2 scenario during the 2nd half of the 21st century. Both the historical and projected climatology were downscaled to 1×1 km spatial resolution by SNAP (2013).

Across the North Slope, the annual mean air temperature has a clear regional pattern (Fig. 3), which generally agrees with the partitioning of bioclimate subzones (Fig. 1b). The annual total incoming shortwave radiation has an increasing trend from west to east across the North Slope. The annual total precipitation has a similar regional pattern to the air temperature, with higher precipitation in the south.

To obtain the day-to-day variation of shortwave radiation, we assumed that the difference between daily values and the monthly mean follows a generalized extreme value distribution (Coles 2001). We then fit the distribution to satellite-based solar radiation from the National Solar Radiation Database (NSRDB, Wilcox 2012) at 12 sites on the North Slope of Alaska (Table A1; Fig. A1). At each of the 12 sites, we calibrated a unique set of parameters for each month. Using the same method, we estimated variations of daily maximum and minimum air temperature, based on measured air temperature at 25 NCDC (National Climatic Data Center, <http://www.ncdc.noaa.gov/>) sites (Table A2, Appendix A1). At each of the 25 sites, we calibrated one set of parameters for each month. We used a distance-weighted method to determine which site's parameters for daily radiation, maximum and minimum air temperature were used for each specific 1×1 km grid pixel across the region. Then we used the monthly value from the SNAP dataset and the fitted distributions here to obtain the daily climate forcing data that drove the model.

Modeling protocol

The MEL model was calibrated by Pearce et al. (2015) to match annual C, N, P and water fluxes near Toolik Lake on the North Slope of Alaska ($68^\circ 38'N$, $149^\circ 43'W$). Although species composition is not explicitly represented in the MEL model, the effects of changes in species composition have been incorporated into the allometry equations, which partitions vegetation into woody and active biomass; all four of the major tundra types (moist tussock, heath, shrub, and wet sedge) fit along this allometric function (Pearce et al. 2015). In addition, we have shown empirically that

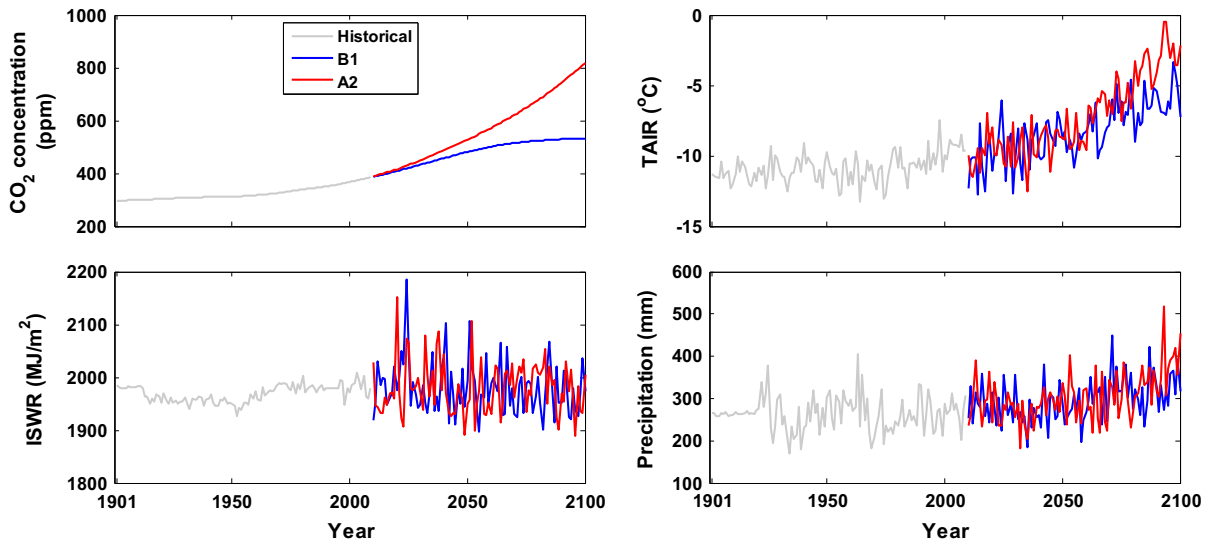


Fig. 2 Time series of historical (1901–2009, CRU.TS31) and future (2010–2100, ECHAM5 B1 and ECHAM5 A2) climate data used to drive the MEL simulations. TAIR: air temperature; ISWR: incoming shortwave radiation

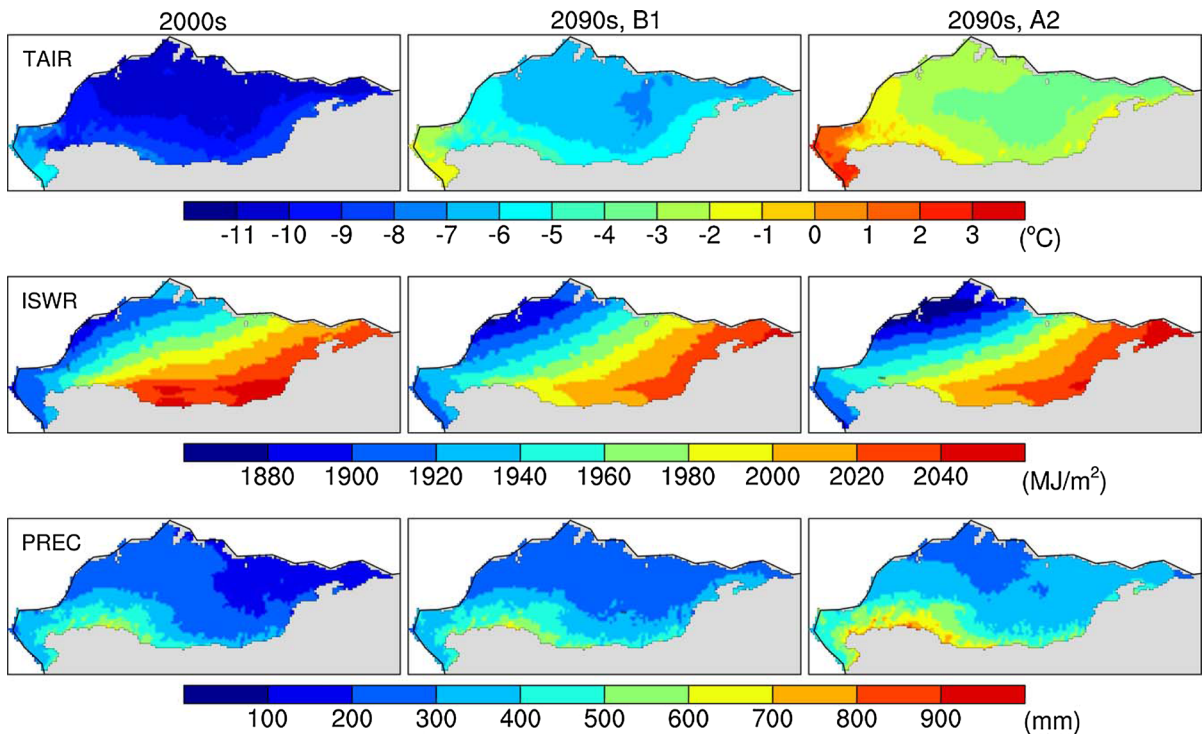
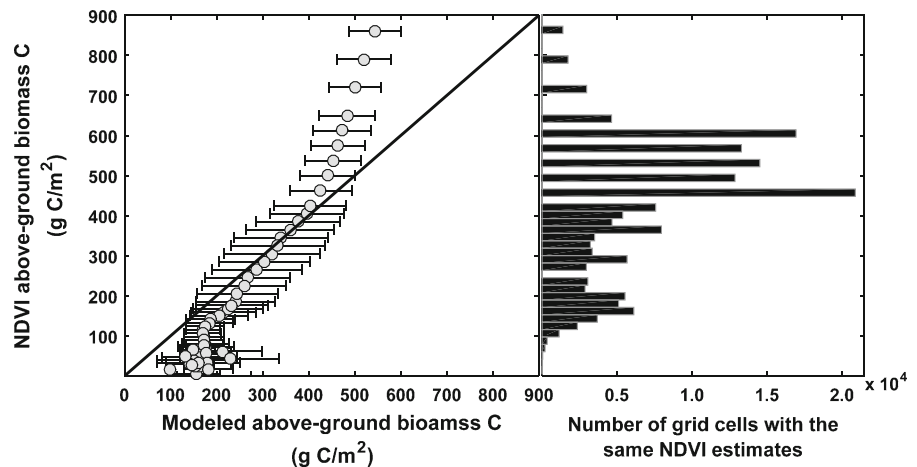


Fig. 3 The spatial distribution of the averaged annual air temperature (*TAIR*), incoming shortwave radiation (*ISWR*) and precipitation (*PREC*) data in 2000s (2000–2009), 2090s (2090–2099) from the B1 scenario, 2090s from the A2 scenario across the North Slope

whole-canopy photosynthesis for all tundra types across the Arctic can be predicted from leaf area, air temperature, and photon flux density using a single equation

with a single set of parameters (Shaver et al. 2007; Street et al. 2007, 2012). We are therefore confident that the MEL model can be used to represent the diversity of

Fig. 4 MEL modeled above-ground biomass C (g C/m²) versus the NDVI estimated above-ground biomass C for all 1 × 1 km grid cells of the North Slope. The *black line* represent the 1:1 line, and the *circle* represents the modeled mean values of above-ground biomass C corresponding to each NDVI based estimate



tundra types on the North Slope. Nevertheless, the simulation was limited to the region south of 70.8°N because the parameterization has poor performance for the water-saturated wetland ecosystems above this latitude (the extreme northern tip of Alaska).

Given the lack of data for initial conditions, we ran 1000 years spin-up simulations to set the initial conditions for all state variables in our simulations (i.e., vegetation and soil C, N and P pools). For all of the 1 × 1 km grid cells, we began these spin-up simulations using the vegetation and debris C, N, and P stocks from Pearce et al. (2015), SOM C stocks estimated from the seasonally-thawed “active layer” in Mishra and Riley (2012), and the SOM N and P stocks were determined using SOM C:N and C:P ratios in Pearce et al. (2015). We then partitioned SOM into phase I and II based on the fractions in Pearce et al. (2015). During the spin-up period, the 1901–1910 climate data were repeated consecutively to drive the model to allow vegetation and soil processes to achieve steady state. Thereafter, the model was driven by the transient climate data (1901–2100). The MEL simulations were conducted for the North Slope of Alaska ($\sim 1.7 \times 10^5$ km²) at 1 × 1 km spatial resolution.

GIS data

We compared our modeled biomass estimates to the satellite estimates of above-ground biomass (Fig. 4), which is based on an exponential relationship between the Normalized Difference Vegetation Index (NDVI) and aboveground plant biomass (phytomass) calculated from clip harvest data (Walker et al. 2003; Fig. 1d). We used the vegetation map (Raynolds et al.

2006, Fig. 1c) to identify the type of vegetation for each 1 × 1 km pixel. Then we multiplied our modeled total biomass C by the ratio of above-ground to total biomass for each of the different vegetation types in Shaver and Chapin (1991) to estimate above ground biomass. We also compared the MEL modeled SOM C stocks across the North Slope with the Northern Circumpolar Soil Carbon Database version 2 (NCSCDv2) (Hugelius et al. 2014).

Partitioning ecosystem C change

Finally, using a modification of the stoichiometric analysis developed by Rastetter et al. (1992; see also McKane et al. 1997), we partitioned changes in regional C stocks into five nutrient-associated factors: (1) net change in total N or P in vegetation plus SOM (including debris); (2) redistribution of N or P between vegetation and SOM; (3) change in vegetation C:N or C:P ratio; (4) change in SOM C:N or C:P ratio, and (5) the interaction of factors 1–4. Using C–N interactions as an example, the equations used to partition changes in regional C stocks were as follows:

$$\Delta C_T = \Delta C_{\Delta N} + \Delta C_{\text{redis}} + \Delta C_{\Delta qV} + \Delta C_{\Delta qSOM} + \Delta C_{\text{inter}}$$

$$\Delta C_{\Delta N} = \Delta N_T \cdot q_T(0)$$

$$\Delta C_{\text{redis}} = [q_V(0) - q_{SOM}(0)] \cdot [\Delta N_V \cdot N_{SOM}(0) - \Delta N_{SOM} \cdot N_V(0)] / N_T(0)$$

$$\Delta C_{\Delta qV} = N_V(0) \cdot \Delta q_V$$

$$\Delta C_{\Delta qSOM} = N_{SOM}(0) \cdot \Delta q_{SOM}$$

$$\Delta C_{\text{inter}} = \Delta N_V \cdot \Delta q_V + \Delta N_{SOM} \cdot \Delta q_{SOM}$$

where ΔC_T , $\Delta C_{\Delta N}$, ΔC_{redis} , $\Delta C_{\Delta qV}$, $\Delta C_{\Delta qSOM}$, and ΔC_{inter} are the changes in total ecosystem C associated with factors 1–5. N_T , N_V and N_{SOM} are total ecosystem N, vegetation N and SOM N, respectively. q_V , q_{SOM} , and q_T are vegetation, SOM, and total ecosystem C:N ratios, respectively. Here, “0” represents the “initial”, and “ Δ ” represents the change since the “initial”. This partitioning scheme is based on the fact that all organisms require C, N, and P, and there were limits to the allowable ranges of C:N and C:P ratios within organs, organisms, and communities (Shaver et al. 1992).

Results

Model performance

MEL modeled above-ground biomass C explained 59 % ($R^2 = 0.59$, $RMSE = 112 \text{ g C/m}^2$) of the spatial variation of the estimated above-ground biomass C derived from the Toolik-Arctic Geobotanical Atlas (Fig. 1d. Grouped by the vegetation types in Fig. 1c, our model successfully simulated above-ground biomass in different vegetation types without using any species-specific information in the model parameterization

(Fig. 5). Compared with the estimated above-ground biomass C derived from the remote sensed NDVI (Walker et al. 2003), differences occurred in the areas dominated by low shrub and moist tussock, where MEL model produced slightly lower above-ground biomass C stocks (Fig. 5). The gridded NDVI biomass data was the only corroboration we had because we used the only soil data to initialize the spin-up simulation. Changes in SOM in our simulations were on the order of about 1–2 %, which would be too small to detect in any dataset. These changes were small for SOM pool but had large effects on vegetation, where they were detectable and where our model appeared to do well.

C fluxes and stocks

The steady-state regional C stock was $\sim 3451 \text{ Tg}$, of which 93 Tg was stored in vegetation biomass, 68 Tg in debris, 684 Tg in Phase I SOM, and 2607 Tg in Phase II SOM (Table 1). Over the historical simulation (1901–2009), regional C stocks had no significant trends in the first seven decades, and then increased over the last three decades of the 20th century (Fig. 6). By 2000, vegetation biomass C increased by 18.0 Tg C (19.5 %) and debris by 5.1 Tg C (7.5 %), but Phase I SOM decreased by 3.9 Tg C (0.6 %) and Phase II SOM decreased by 9.2 Tg C (0.4 %) relative to the

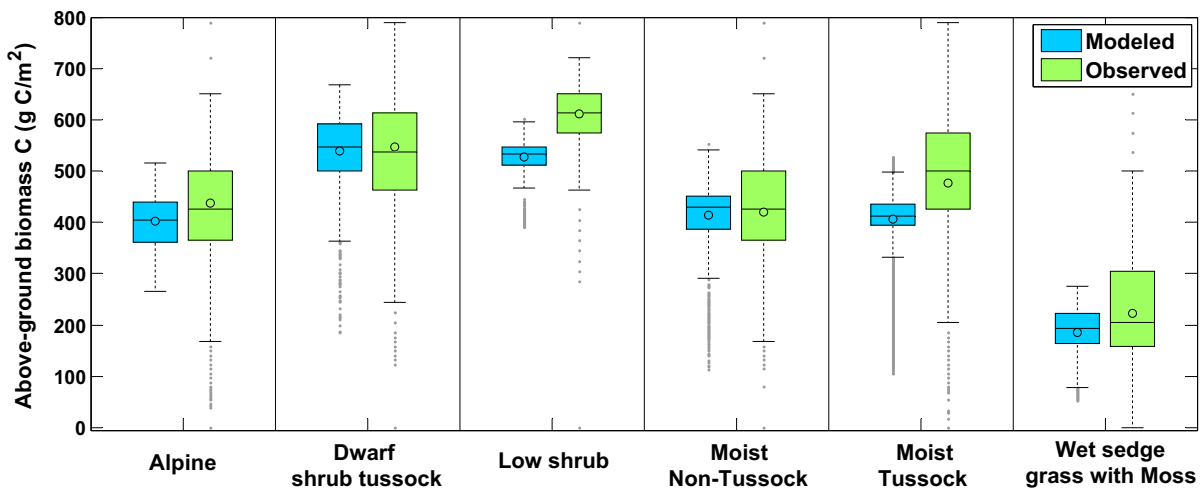


Fig. 5 Above-ground vegetation biomass C stocks in areas dominated by different vegetation types. The vegetation map used to match the vegetation types is derived from Reynolds et al. (2006) as shown in Fig. 1. The observed biomass C stocks are derived from the Toolik-Arctic Geobotanical Atlas (<http://www.arcticatlas.org/>) as shown in Fig. 1, with an assumption

that C accounts for 50 % of dry weight of biomass. For the MEL modeled biomass C, we used the portions of above-ground biomass to total biomass demonstrated in Shaver and Chapin (1991). For Alpine tundra and moist non-tussock tundra, we used the same portion for shrub in Shaver and Chapin (1991)

Table 1 Modeled C, N and P storages and C:N, C:P ratios in biomass, debris, Phase I and II soil organic matter and the total ecosystem

		1900	2000s (2000–2009)	2090s (2091–2099) under B1	2090s (2091–2099) under A2
Biomass	C (Tg)	92.5	110.5	138.4	164.8
	N (Tg)	1.85	2.12	2.51	2.80
	P (Tg)	0.196	0.228	0.276	0.317
	C:N	49.9	52.2	55.2	58.7
	C:P	471	485	502	520
Debris	C (Tg)	67.8	72.9	78.4	82.9
	N (Tg)	0.88	0.95	1.02	1.08
	P (Tg)	0.088	0.095	0.102	0.108
	C:N	76.9	76.9	76.9	76.9
	C:P	769	769	769	769
Phase I soil organic matter	C (Tg)	684.2	680.3	671.7	671.1
	N (Tg)	23.88	23.82	23.56	23.00
	P (Tg)	2.214	2.216	2.222	2.176
	C:N	28.7	28.6	28.5	29.2
	C:P	309	307	302	308
Phase II soil organic matter	C (Tg)	2606.8	2597.6	2592.8	2593.3
	N (Tg)	121.24	120.82	120.59	120.62
	P (Tg)	14.896	14.843	14.816	14.819
	C:N	21.5	21.5	21.5	21.5
	C:P	175	175	175	175
Ecosystem	C (Tg)	3451.4	3461.4	3481.4	3512.1
	N (Tg)	147.86	147.71	147.68	147.50
	P (Tg)	17.395	17.382	17.416	17.419
	C:N	23.3	23.4	23.6	23.8
	C:P	198	199	200	202

steady state (Table 1). Driven by the B1 and A2 climate, the vegetation C stocks increased respectively 25 % (+27.9 Tg C) and 50 % (+54.3 Tg C) over the 21st century. Along with the biomass increase, more litter production led to respectively 8 % (+5.5 Tg C) and 14 % (10.0 Tg C) higher debris C pools under the B1 and A2 climate. The increased biomass had higher photosynthetic potential (i.e. GPP), which increased from 442.6 to 568.5 g C/m²/year during the 21st century under the B1 climate, and increased to 711.7 g C/m²/year under the A2 climate (Fig. 7). The increase in air temperature also enhanced ecosystem respiration (plant respiration plus soil respiration). In particular, the ecosystem respiration increased from 436.4 to 556.5 g C/m²/year during the 21st century under the B1 climate and increased to 711.1 g C/m²/year under the A2 climate (Fig. 7). Consequently, the total SOM

C stock (Phase I plus Phase II) lost about 13.4 (0.4 %) and 13.5 (0.4 %) Tg C under the B1 and A2 climate, respectively. Overall, the higher increase in vegetation and debris C stocks than the decrease in SOM C stock led to 20.0 (0.6 %) and 50.7 (1.5 %) Tg net C gain in the total regional C stocks under the B1 and A2 climate, respectively (Fig. 6).

Across the North Slope, the distribution of both vegetation and SOM C stocks had large spatial variations (Fig. 8a) and there was a strong positive correlation between the two ($R^2 = 0.68$). Across the North Slope, SOM C stocks of the annually thawed active layer ranged from 10 to 26 kg C/m² in 2000 (Fig. 8a). This range was within the range of the Northern Circumpolar Soil Carbon Database version 2 (NCSCDv2) (Hugelius et al. 2014), which is from 1 to 24 kg C/m² for the top 30 cm depth, and from 1 to

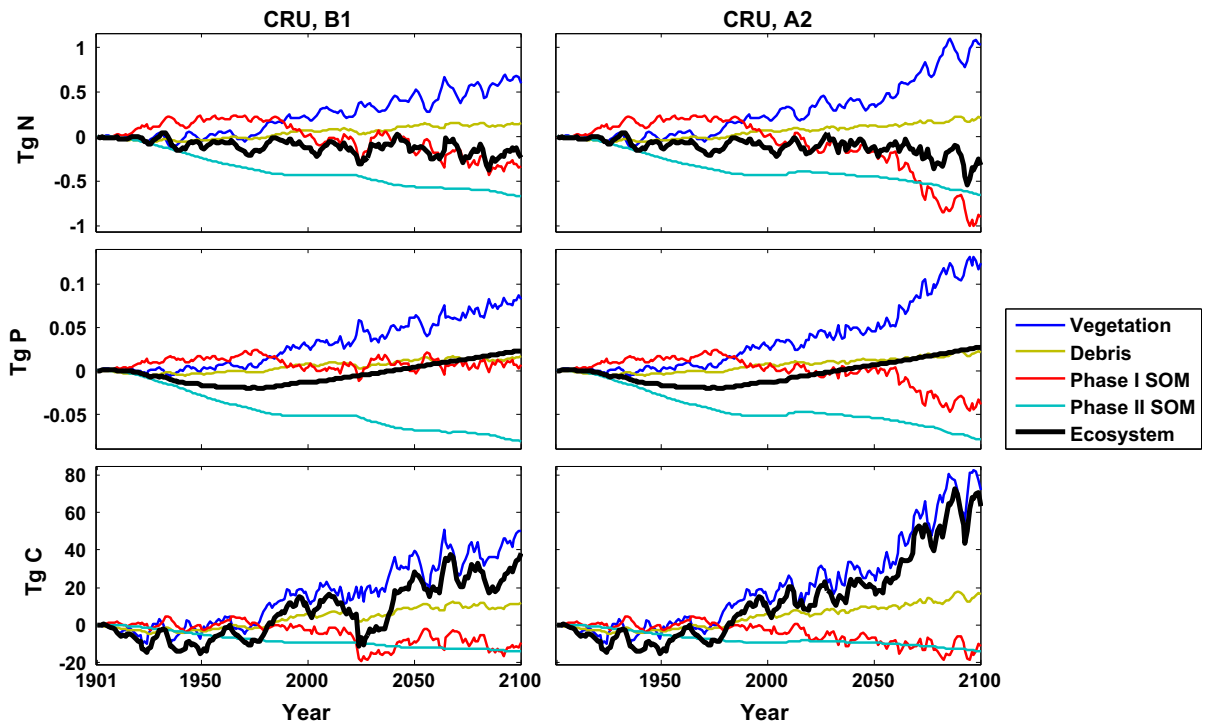


Fig. 6 The simulated change of N, P and C stocks in vegetation, debris, Phase I and Phase II SOM from 1901 to 2100, under the historical (*CRU*) and future (*B1* and *A2*) climate data

66 kg C/m² for the top 100 cm depth; much of the deeper C would be below the permafrost table. Vegetation C stock ranged from 0.2 to 0.9 kg C/m² with relatively low values in the northern coastal area because of the low air temperature (Fig. 8a). Both the B1 and A2 climates caused losses of SOM C by as much as 300 g C/m² in most parts of the North Slope, except the northern coastal area where SOM C increased by as much as 300 g C/m². Overall, the warming climate contributed to a larger vegetation C pool, and both the B1 and A2 climates led to a net gain in ecosystem C stocks in most parts of the North Slope (Fig. 8a). However, the spatial variation of vegetation C had very low correlation with air temperature. Based on a linear regression, the spatial variation of annual mean air temperature only accounted for 6 % of the spatial variation in vegetation C.

N fluxes and stocks

The steady-state regional N stock was ~147.9 Tg, of which 1.9 Tg was stored in vegetation biomass, 0.9 Tg in debris, 23.9 Tg in Phase I SOM, and 121.2 Tg in

Phase II SOM (Table 1). Over the historical simulation (1901–2009), the N mineralization rate had no significant trend before 1970s, but had a clear increasing trend from then on (Fig. 7). This increase in mineralization reduced the N stock of Phase II SOM (Fig. 6). Meanwhile, the plant N uptake rate was generally lower than the N mineralization rates, and inorganic N was lost from the system through leaching. Given the very small external N inputs (i.e. N deposition and fixation), leaching of N resulted in a net loss from the region (~0.15 Tg or ~0.1 %), which consisted of a 0.27 Tg increase in vegetation N, a 0.07 Tg increase in debris N, a 0.06 Tg decrease in phase I SOM N, and a 0.42 Tg decrease in phase II SOM N (Fig. 6).

Over the 21st century, N mineralization rates increased from 4.71 to 5.54 g N/m²/year under the B1 climate, and to 6.40 g N/m²/year under the A2 climate (Fig. 7). The consequent increase in plant available N allowed faster plant N uptake. Quantitatively, over the century, plant N uptake increased from 4.66 to 5.44 g N/m²/year under the B1 climate, and increased to 6.18 g N/m²/year under the A2 climate. As in the latter part of the 20th century, higher N

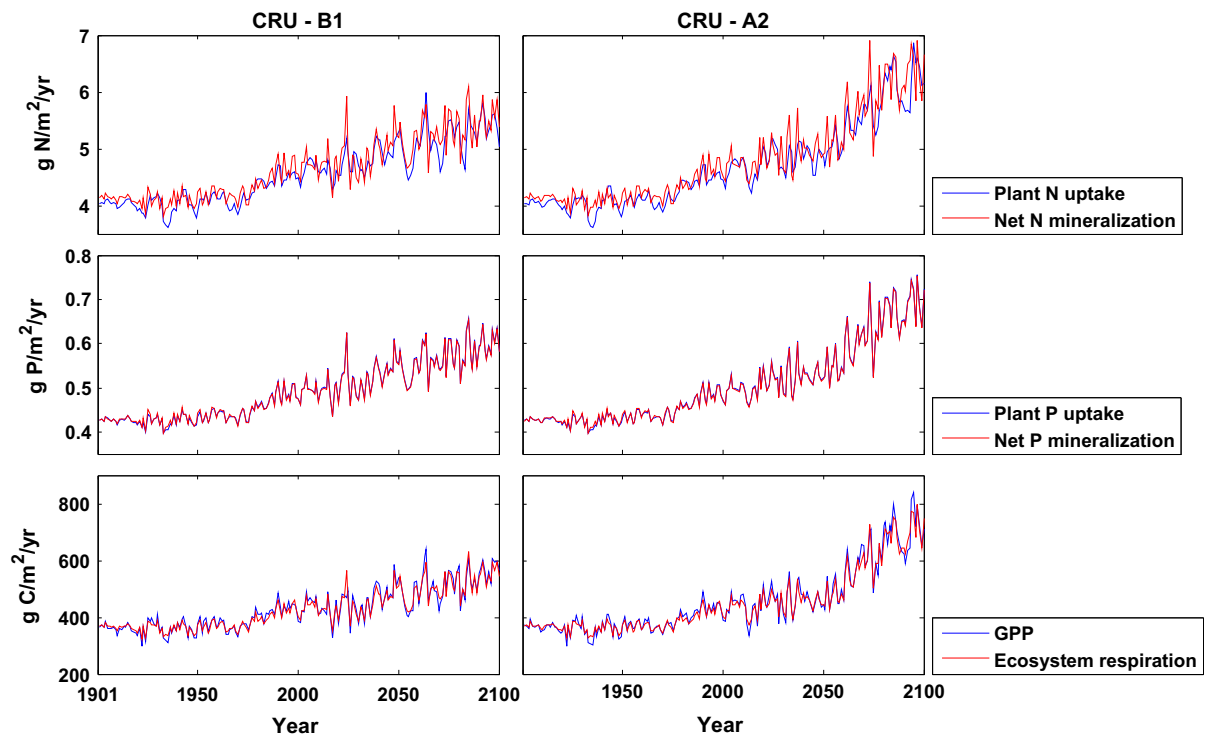


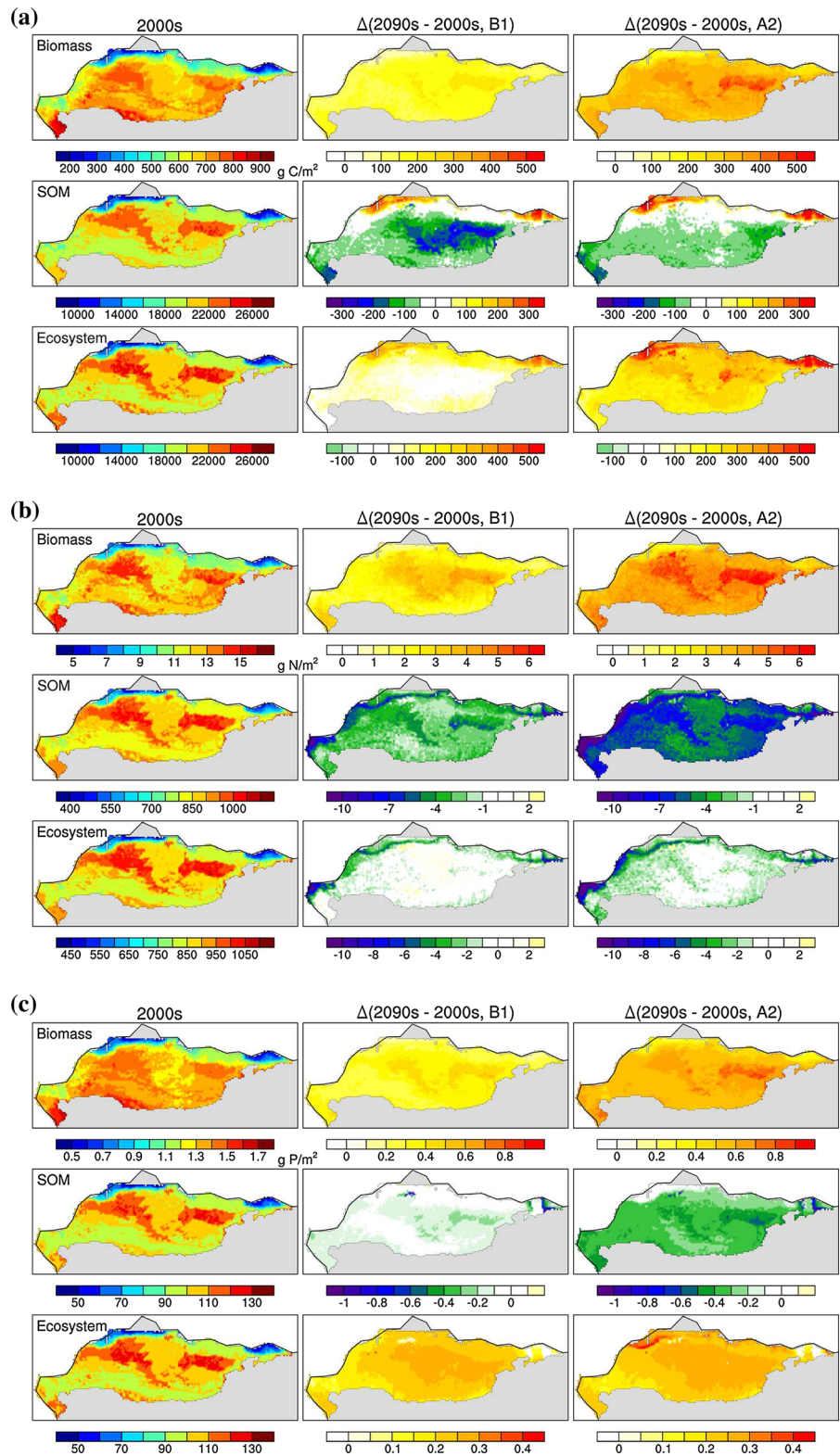
Fig. 7 The modeled N (net N mineralization and plant N uptake), P (net P mineralization and plant P uptake) and C (GPP and ER) fluxes driven by the historical (*CRU*) and future (*B1* and *A2*) climate data

mineralization rates than N uptake rates caused a buildup of inorganic N and subsequent leaching losses during the 21st century; the external N supply (i.e. N deposition and fixation) was too small to compensate for these losses. As a result, the regional N stock decreased by 0.03 and 0.21 Tg N (0.02 and 0.14 %) under the B1 and A2 climate, respectively. All of these losses of N were from phase I and II SOM (i.e. B1: -0.49 ; A2: -1.02 Tg N), which were only partly compensated by increases of N in vegetation and debris (i.e. B1: $+0.46$; A2: $+0.81$ Tg N, Table 1).

The SOM N stock was spatially heterogeneous across the North Slope and reflected the SOM N stock used to initialize the model (Fig. 8b). Generally, the SOM N pool had unimodal north–south distribution with the highest values in the northern foothills and decreasing from there toward both the mountains to the south and the coast to the north. In 2000, the SOM N stock ranged from 400 to 1200 g N/m² across the North Slope. The vegetation N stock had strong positive correlation with the SOM N stock but weak positive correlation with air temperature. In particular,

the SOM N stock accounted for 74 % of the spatial variation of biomass N stock from simple linear regression, whereas the air temperature accounted for only 5 %. By 2000, the vegetation N stock in our simulations ranged from 4 to 17 g N/m² across the North Slope (Fig. 8b). Because the SOM N stock accounted for more than 95 % of the total ecosystem N, the spatial variations and magnitudes of total ecosystem N stock followed the spatial patterns of SOM N distribution across the region. Both the B1 and A2 climates led to net loss in SOM N stock in most parts of the North Slope, with greater warming corresponded to greater nutrient losses (Fig. 8b). The spatial variation of SOM N stock was large and areas with higher initial SOM N pool had larger SOM N loss under the warming climates. Over the 21st century, climate warming resulted in a -10 to $+2$ g N/m² change in SOM N stocks across the North Slope. Most of the N released from the SOM pool was acquired by the vegetation; therefore the spatial pattern of increases in vegetation N stocks was well correlated to decreases in SOM N stocks (Fig. 8b).

Fig. 8 Modeled North Slope **a** C, **b** N and **c** P stocks in biomass, SOM and the total ecosystem in 2000s (2000–2009), and the differences between 2090s (2090–2099) and 2000s under the two projected future climate data (*B1* and *A2*)



P fluxes and stocks

The steady-state regional P stock was ~ 17.4 Tg, of which 0.2 Tg was stored in vegetation biomass, 0.09 Tg in debris, 2.2 Tg in Phase I SOM, and 14.9 Tg in phase II SOM (Table 1). The MEL model simulated a net 0.01 Tg P or 0.06 % loss from the system between 1901 and 2009, which consisted of a 0.03 Tg increase in vegetation P, a 0.01 Tg increase in debris P, no change in phase I SOM P, and a 0.05 Tg decrease in phase II SOM P stock (Fig. 6). Under warming climate, P mineralization and uptake rates had similar increasing trends as those of N (Fig. 7). However, unlike the N fluxes, where net mineralization rates clearly increased more than plant uptake rates, plants absorbed nearly all of the P mineralized from the SOM pool plus additional P input into the ecosystem through weathering and deposition. There was therefore a net gain in ecosystem P stocks under both projected warming climates (Fig. 6). Over the 21st century, the regional P stocks increased 0.034 Tg (0.20 %) under the B1 climate. This increase was distributed among vegetation biomass (+0.048 Tg P), debris (+0.007 Tg P) and phase I SOM (+0.006 Tg P) and was only partly compensated by P loss from phase II SOM (−0.027 Tg P, Table 1). Under the A2 climate, the regional P stock increased 0.038 Tg (0.22 %), which was distributed between vegetation biomass (+0.089 Tg P) and debris (+0.013 Tg P), but partially compensated by decreases of P in phase I (−0.040 Tg P) and II SOM (−0.024 Tg P, Table 1).

The spatial distribution of SOM P stock was similar to the SOM N stock (Fig. 8c). By 2000, the SOM P stock on our simulations ranged from 40 to 140 g P/m² across the North Slope. As with the biomass N stock, the biomass P stock had a strong positive correlation with SOM stocks but weak positive correlation with air temperature. By 2000, vegetation P stock ranged from 0.4 to 1.8 g P/m² across the North Slope (Fig. 8c). The spatial variations and magnitudes of total ecosystem P stock followed the spatial patterns of SOM P distributions across the region. Both the B1 and A2 climates led to net loss in SOM P stock in most parts of the North Slope, with increased warming leading to increased nutrient losses (Fig. 8c). Spatial variation of SOM P stock was large and areas with higher initial SOM P pool had larger SOM P loss under the warming climates. Over the 21st century, climate warming resulted in a −1 to +0.1 g P/m² change in

SOM P stocks across the North Slope. Most of the P released from the SOM pool was acquired by the vegetation; therefore the spatial pattern of increases in vegetation P stocks was well correlated to decreases in SOM P stocks (Fig. 8c).

Partitioning ecosystem C change into C–N and C–P based interactions

Under the B1 scenario with moderate emissions and warming, the net loss of regional N over the 200-year simulation would result in about 6 Tg net reduction in regional C, all other factors remaining constant (ΔN Fig. 9). About 16 Tg C accumulation in the region can be attributed to the redistribution of N from SOM, with a low C:N, to vegetation, with a higher C:N (N redistribution in Fig. 9). The increase in vegetation C:N (e.g., due to increases in abundance of woody tissues relative to leaves and fine roots) contributed ~ 15 Tg increase in regional C ($\Delta C:N$ Vegetation Fig. 9). The increased C:N ratio of SOM resulted in ~ 8 Tg C gain in regional C stocks over the 200 years ($\Delta C:N$ SOM Fig. 9). The interaction of the four factors contributed an additional 5 Tg C (interaction Fig. 9). Under the high emissions and warming A2 scenario, carbon flux and stock changes had similar patterns to those under the B1 scenario, but with larger magnitudes (Fig. 9).

Using the same partitioning method, analysis based on C–P interactions yielded contrasting results. Under the B1 scenario, the net accumulation of regional P over the 200 years resulted in a 5 Tg C net gain in regional C (ΔP Fig. 9). The redistribution of P from SOM, with a low C:P, to vegetation, with a higher C:P (P redistribution in Fig. 9), resulted in 23 Tg C accumulation. Increased vegetation C:P led to 8 Tg C increase in regional C stocks ($\Delta C:P$ Vegetation) and the slight increase in SOM C:P ratio resulted in almost no change to the regional C stocks by 2100 ($\Delta C:P$ SOM Fig. 9). The interaction of the four P-associated factors contributed an additional 3 Tg C (interaction Fig. 9).

Differences between the N-based and P-based partitioning of the net changes in regional C existed for all four factors: (1). The net decrease in total ecosystem N led to loss in regional C, while the net increase in total ecosystem P led to gain C by 2100. This difference was ~ 10 Tg C under the B1 climate and 13 Tg C under the A2 climate. (2) The

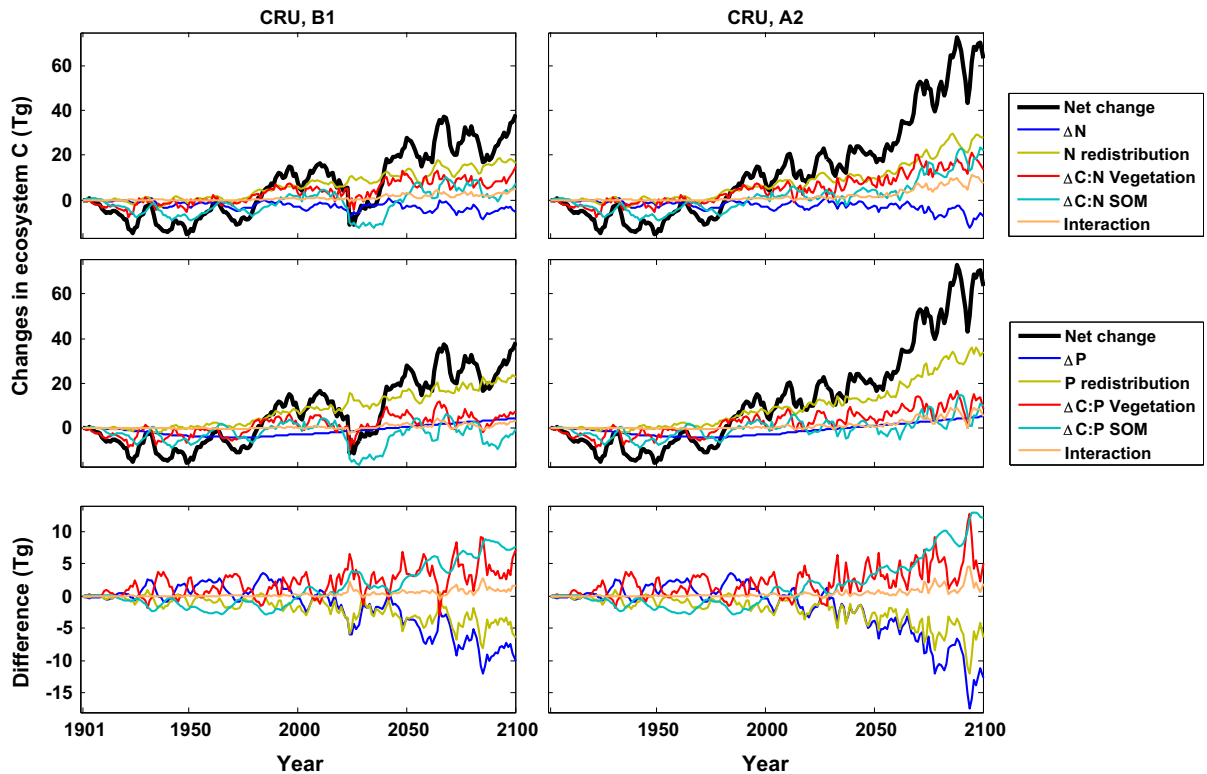


Fig. 9 Simulated net change in ecosystem C stocks partitioned among three biogeochemical factors and their interaction at three sites from 1901 to 2100 for the whole North Slope of Alaska. The bottom pattern shows the difference (g/m^2) between the N partitioning and the P partitioning in panels above. “ ΔN ” or “ ΔP ” indicates a change in C stocks associated with a change

in the total N or P in the ecosystem; “ $\Delta\text{C:N}$ ” or “ $\Delta\text{C:P}$ ” is the change associated with changes in the C:N or C:P ratios of vegetation or soil (SOM), “N redistribution” or “P redistribution” is the change associated with the redistribution of N or P among pools, and “interaction” is the change associated with the interaction of all three factors

redistribution of N from SOM to plants resulted in 6 Tg lower increase in regional C than the redistribution of P from SOM to plants under both B1 and A2 climates. (3) The increase in vegetation C:N ratio led to higher regional C gain in comparison to the increase in vegetation C:P. This difference was ~ 7 Tg C under the B1 and ~ 5 Tg C under the A2 scenario. (4) The increase in SOM C:N ratio caused larger gain in regional C than did the increase in SOM C:P; the difference was 8 Tg C under the B1 scenario and 12 Tg C under the A2 scenario (Fig. 9).

Discussion

We used a model developed and tested with plot-scale data to examine the spatial patterns of plant and soil C, N, and P stocks across the North Slope of Alaska and

to explore how those stocks might change in response to climate warming. Our modeled spatial variation of vegetation C stocks generally agreed with biomass estimates derived from satellite NDVI. Compared with the NDVI biomass, our model results had clear biases at the high and low end, but those NDVI values are very rare. Moreover, as clarified in Walker et al. (2003), there is considerable uncertainty regarding biomass of NDVI values above about 0.55 (~ 641 g C/m^2) because of the non-linear relationship between NDVI and biomass. Therefore, it is possible that our results were more close to the real biomass amount in those highly vegetated areas. Our modeled ranges of the present-day SOM C pool (10–26 kg C/m^2) was within the range of empirical data (NCSCDv2) (Hugelius et al. 2014). The model-data difference between our modeled SOM C and the NCSCDv2 SOM C can be partly attributed to environmental variations

that have not been explicitly captured in our historical simulations (e.g., thermal erosion, changes in active layer thickness). However, considering the scarce data and limited representation of spatial heterogeneity for the North Slope, rigorous tests of the modeled SOM predictions are simply not possible. We acknowledged that the quantitative predictions of the model in relation to the magnitude, timing, and location of changes should be used with extreme caution. Instead, we emphasized the qualitative results on how and why the tundra will change.

Nutrient limitation under warming climate

Increased air temperature stimulates mineralization of the SOM pool, thereby leading to more plant available nutrients. Although the Phase II SOM had low nutrient turnover rates, it still provided the major source for mineralization simply because its pool size was large. The consequent higher concentration of plant available N (i.e. NH_4^+ , NO_3^- , DON) and P (i.e. PO_4^{3-}) in soil allowed faster plant uptake rates, faster growth and litter production rates, which helped maintain Phase I SOM element stocks. Over the 200-year simulations, N mineralization rate was greater than plant N uptake rates (Fig. 7) and N was lost from the system through leaching. Meanwhile, the tighter linkage between P mineralization and uptake rates indicated that P release is still not sufficient to fulfill the plant requirement and P was tightly retained by the plants. Because the rate of plant growth is constrained only by the supply rate of most limiting resource needed for growth (Loladze et al. 2000; Grover 2004; Haefner 2005; Rastetter 2011), long-term tundra plant growth under warming climate is predicted to be P-limited unless a mechanism exists to increase the P supply to the ecosystem (e.g., biologically enhanced weathering, Rastetter et al. 2013). It should also be noted that N is very limiting in tundra on the North Slope. There is therefore very little or no nitrification–denitrification (Giblin et al. 1991; Nadelhoffer et al. 1991; Shaver et al. 1992; Mack et al. 2004; Yano et al. 2010). Thus, NO_x losses should be negligible and very localized (e.g., riparian fringe).

Plot scale analyses of tundra recovery from fire and thermokarst using the MEL model indicate that the post-disturbance recovery of tundra vegetation is predominantly N limited (Pearce et al. 2015; Jiang et al. 2015). These earlier results appear to contradict

the implication of P limitation by the stronger P retention than N retention with warming in the simulations presented here. However, the earlier results reflect a predominantly plant response to fertilization; the results here reflect the overall accumulation of N and P by the whole ecosystem. The ratio of N:P accumulated in the whole ecosystem in our simulations here is simply lower than the N:P ratio in the inputs used to drive the model. Moreover, N and P are the most limiting nutrients in this system (Shaver and Chapin 1980; Shaver et al. 2001, 2006). Nutrient limitation by secondary nutrients such as calcium (Ca) and magnesium (Mg) are not likely to play a large role in the arctic due to the order of magnitude lower C:Ca or C:Mg in arctic plants.

Varied trends of C and nutrient budgets

The long-term climate warming stimulates a net transfer of nutrient (i.e. N and P) from SOM (low C:nutrient ratio) to vegetation (high C:nutrient ratio), and changes in biomass and SOM C:nutrient ratios. These warming-caused changes in C, N, and P interactions (Fig. 9) result in a larger vegetation C stock that offsets decreases in the SOM C stock. Therefore, the ecosystem gains C under a warmer climate (Fig. 6). The large modeled increase in vegetation C stock associated with warming agrees with both field experimental and remotely-sensed observations in the North Slope (Chapin et al. 1995; Chapin and Shaver 1996; Shaver and Jonasson 1999; Stow et al. 2004; Goetz et al. 2005; Verbyla 2008). The slight reduction in SOM C is consistent with the findings in a 20-year greenhouse experiment by Sistla et al. (2013), but is much smaller than the SOM C decrease in response to the 20-year nutrient fertilization in Mack et al. (2004).

Constrained by the allowable ranges of C:nutrient ratios within plant tissues, species, and communities (Shaver et al. 1992), a new C-nutrient distribution will be the result of altered vegetation structure and composition (e.g., higher woody dominance) in future tundra ecosystems. The increases in vegetation C:nutrient ratio can be due either to an accumulation of high C:N or high C:P biomass (e.g., stem and rhizomes) or a shift of vegetation cover to species with these properties (e.g., shrubbier tundra, Rustad et al. 2001; Walker et al. 2006; Myers-Smith et al. 2011). The increased C:nutrient ratio in vegetation

biomass will lead to further increase in SOM C:nutrient ratio through low quality (high C:nutrient) litter input to the soil. This C-rich substrate mineralizes N and P more slowly because of microbial retention and immobilizes nutrients more strongly, thus reducing availability of N and P for plant uptake in the future tundra ecosystem.

Additional insight into the future control on C stock in Alaska tundra can be derived from the comparison of C–N and C–P interactions (Fig. 9). Differences between the N-based and P-based partitioning of changes in regional C stock indicate that the distinctly different patterns of N and P cycles in response to warming have remarkably different impacts on C stocks. Relative to N, P is more tightly cycled in the system; therefore changes in regional C stocks are more sensitive to the net change or redistribution of P (Fig. 9). In contrast to P, N released from soil cannot be fully taken up by plants, and N loss through leaching can be accounted for the difference of C stock changes associated with N and P redistribution from soil to vegetation, and the difference associated with the net change in N and P stocks in the region. Therefore, we predict that the availability of plant available P has a stronger effect on determining the future C stock in Alaska tundra.

Causes for the spatial variation

The spatial variation of our modeled SOM C and nutrient stocks are strongly influenced by the SOM map used to initialize the simulation. According to Mishra and Riley (2012), areas of higher SOM C stocks were primarily associated with wet soils (low slope, large upslope catchment area), while areas of lower SOM stocks were primarily associated with dry upper slopes. Compared to the initial SOM C map (Mishra and Riley 2012), the model underestimates SOM in the northern wetland area. This is probably because our model lacks a good representation of topographic controls on soil texture, moisture, and anoxia, which regulate soil C accumulation in peatlands (Fan et al. 2008). Moreover, the current parameterization based on moist tussock tundra might not be appropriate for the biogeochemical processes in northern wetlands.

Because arctic tundra is a nutrient-limited system and the major source of nutrients to the vegetation is from the SOM, the spatial variation in SOM pools

strongly influence the spatial variation in vegetation biomass. In areas with low SOM stocks, there are less nutrients to redistribute from SOM to vegetation and the warming effect on plant growth will be greatly constrained. Climate variability also influences the spatial variation of vegetation biomass. Following the gradient of bioclimate subzones (Fig. 1b), vegetation in the south (warmer than the north) is expected to have higher biomass, as long as the soil nutrient pool can support the plant nutrient uptake requirement. However, our analysis indicates that the spatial variation of annual mean air temperature only accounts for a small portion of the spatial variation in vegetation biomass. The effect of spatial differences in temperature is overwhelmed by the effects of nutrient supply from SOM. Overall, the SOM pool and climate variability together are expected to explain most of the spatial variation in vegetation biomass. Vegetation structure and composition might also impact the spatial variation in biomass more than is allowed by the allometric shifts in our model; but a dynamic vegetation model would be required to simulate these more extreme spatial variations caused by changes in vegetation types under a warming climate.

Uncertainties in modeling future tundra C and nutrient balance

Future tundra C and nutrient balances may depend on other factors that were not considered here. The first uncertainty comes from the external nutrient supply to the system. Because the arctic tundra is strongly nutrient-limited (Shaver and Jonasson 2001; Shaver et al. 2001; Mack et al. 2004), any increase in future N and P inputs might be expected to increase tundra C storage (McKane et al. 1997). However, the present modeling study indicates that the nutrient supply to vegetation in tundra is predominantly controlled by the internal nutrient cycle; the external nutrient inputs (e.g., N deposition, P weathering) are always small (<1 %) relative to internal recycling. Although the N deposition might increase in the arctic region (IPCC 2007), even an order of magnitude increase in deposition should be still much lower than the net N mineralization rate and insufficient to completely offset the N loss through leaching and denitrification. Therefore, the impact of potential increase in N deposition on tundra C budgets should be limited.

However, as climate warms and the annually thawed active layer deepens, additional nutrients (N and P) will be released from thawing permafrost (Hobbie et al. 1999; Frey et al. 2007). The extent to which this release of new nutrients might drive additional plant growth and C accumulation is largely unknown (Schuur et al. 2007).

The second major uncertainty results from the lack of quantitative understanding of major disturbances like wildfire and thermal erosion of permafrost (Rocha et al. 2012). Despite the small frequency of tundra fires in the North Slope, an unprecedented fire event might have considerable impact on the regional C and nutrient budgets. For example, the 2007 Anaktuvuk River fire, which burned more than 1000 km² (Jones et al. 2009), and released ~2.1 Tg C to the atmosphere and 400 years accumulation of N, was large enough to affect annual C and N budgets of the North Slope and perhaps the entire Arctic (Mack et al. 2011). As climate continues to warm, the number, severity, and area burned by large fires is predicted to increase (Hu et al. 2010), and the warming-caused increase in ecosystem C stocks in unburned areas might not be sufficient to compensate large C and N losses from burned areas. Therefore, the net effect of climate warming on arctic tundra C balance needs to be reassessed to include consideration of changes in C, N, and P balance in large burned and otherwise disturbed areas. This work can only be done using models such as the MEL model used in the present study.

Conclusion

Our modeling study indicates that the ongoing warming climate in Arctic enhances mineralization and leads to a net transfer of nutrient from soil organic matter to vegetation, thereby stimulating tundra plant growth and increased C inputs to the tundra ecosystems. Given the small external nutrient supplies (i.e. N deposition and fixation, P weathering) to the system, N and P mineralization rate is the dominant predictor of plant nutrient availability and positively correlates to the magnitude of the warming. As climate warms, the release of N is modeled to be in excess of plant requirement, and N is lost from the system. However, the P will be strongly retained by plant uptake because P is the more limiting nutrient resource in the long run. As the principal source of plant-available nutrients, the

SOM pool strongly determines the spatial variation of vegetation biomass. Under a warming climate, nutrient releases from thawing permafrost and disturbances (e.g., wildfire and thermokarst) might contribute substantial uncertainties to the spatial variation of SOM and vegetation C stocks across the region. Our model provides insight on understanding the effect of tightly cycled N and P on the tundra C budget under long-term warming climate.

Acknowledgments We gratefully acknowledge support from NSF Grants # DEB-1026843, EF-1065587, and OPP-1107707 to the Marine Biological Laboratory, Woods Hole, MA. We acknowledge the use of Alaska Arctic Bioclimate Subzones map, Alaska Arctic Biomass map, and Alaska Arctic Vegetation map derived from the Toolik-Arctic Geobotanical Atlas (<http://www.arcticatlas.org/>).

References

- Belshe EF, Schuur EAG, Bolker BM (2013) Tundra ecosystems observed to be CO₂ sources due to differential amplification of the carbon cycle. *Ecol Lett* 16:1307–1315
- Callaghan TV, Björn LO, Chapin FS III, Chernov Y, Christensen TR, Huntley B, Ims RA, Johansson M, Jolly D, Jonasson S, Matveyeva N, Oechel WC, Panikov N, Shaver GR, Elster J, Henttonen H, Jónsdóttir IS, Laine K, Schaphoff S, Sitch S, Taulavuori E, Taulavuori K, Zöckler C (2005) Arctic tundra and polar desert ecosystems. Arctic climate impact assessment (ACIA). Cambridge University Press, Cambridge, pp 243–352
- Chapin FS III, Shaver GR (1996) Physiological and growth responses of arctic plants to a field experiment simulating climatic change. *Ecology* 77:822–840
- Chapin FS III, Bloom AJ, Field CB, Waring RH (1987) Plant responses to multiple environmental factors. *Bioscience* 37:49–57
- Chapin FS III, Shaver GR, Giblin AE, Nadelhoffer KJ, Laundre JA (1995) Responses of arctic tundra to experimental and observed changes in climate. *Ecology* 76:694–711
- Coles SG (2001) An introduction to statistical modeling of extreme value. Springer, New York
- Fan Z, Neff JC, Harden JW, Wickland KP (2008) Boreal soil carbon dynamics under a changing climate: a model inversion approach. *J Geophys Res* 113:G04016
- Frey K, McClelland J, Holmes R, Smith L (2007) Impacts of climate warming and permafrost thaw on the riverine transport of nitrogen and phosphorus to the Kara Sea. *J Geophys Res-Biogeosci* 112:G04S58
- Friedlingstein P, Cox P, Betts R, Bopp L, Von Bloh W, Brovkin V, Zeng N (2006) Climate–carbon cycle feedback analysis, results from the C4MIP model intercomparison. *J Clim* 19:3337–3353
- Giblin AE, Nadelhoffer KJ, Shaver GR, Laundre JA, Mckerrow AJ (1991) Biogeochemical diversity along a riverside toposequence in arctic Alaska. *Ecol Monogr* 61:415–435

- Giblin AE, Laundre JA, Nadelhoffer KJ, Shaver GR (1994) Measuring nutrient availability in arctic soils using ion exchange resins. *Soil Sci Soc Am J* 58:1154–1162
- Goetz SJ, Bunn AG, Fiske GJ, Houghton RA (2005) Satellite-observed photosynthetic trends across boreal North America associated with climate and fire disturbance. *Proc Natl Acad Sci USA* 102(38):13521–13525
- Gough L, Wookey PA, Shaver GR (2002) Dry heath arctic tundra responses to long-term nutrient and light manipulation. *Arct Antarct Alp Res* 34:211–218
- Gough L, Moore JC, Shaver GR, Simpson RT, Johnson DR (2012) Above- and belowground responses of arctic tundra ecosystems to altered soil nutrients and mammalian herbivory. *Ecology* 93:1683–1694
- Grover J (2004) Predation, competition and nutrient recycling: a stoichiometric approach with multiple nutrients. *J Theor Biol* 229:31–43
- Haefner JW (2005) Modeling biological systems: principles and applications. Springer, New York
- Hansen J, Sato M, Kharecha P, Russell G, Lea DW, Siddall M (2007) Climate change and trace gases. *Philos Trans R Soc A* 365:1925–1954
- Harris I, Jones PD, Osborn TJ, Lister DH (2014) Updated high-resolution grids of monthly climatic observations—the CRU TS3.10 Dataset. *Int J Climatol* 34:623–642
- Hinzman LD, Bettez ND, Bolton WR, Chapin FS III, Dyurgerov MB, Fastie CL, Griffith B, Hollister RD, Hope A, Huntington HP, Jensen AM, Jia GJ, Jorgenson T, Kane DL, Klein DR, Kofinas G, Lynch AH, Lloyd AH, McGuire AD, Nelson FE, Nolan M, Oechel WC, Osterkamp TE, Racine CH, Romanovsky VE, Stone RS, Stow DA, Sturm M, Tweedie CE, Vourlitis GL, Walker MD, Walker DA, Webber PJ, Welker JM, Winker KS, Yoshikawa K (2005) Evidence and implications of recent climate change in northern Alaska and other Arctic regions. *Clim Change* 72:251–298
- Hobara S, McCalley C, Koba K, Giblin AE, Weiss MS, Gettel GM, Shaver GR (2006) Nitrogen fixation in surface soils and vegetation in an Arctic tundra watershed: a key source of atmospheric nitrogen. *Arct Alp Antarct Res* 38:363–372
- Hobbie JE, Peterson BJ, Bettez N, Deegan L, O'Brien WJ, Kling GW, Kipphut GW, Bowden WB, Hershey AE (1999) Impact of global change on the biogeochemistry and ecology of an arctic freshwater system. *Polar Res* 18:207–214
- Hobbie SE, Schimel JP, Trumbore SE, Randerson JR (2000) Controls over carbon storage and turnover in high-latitude soils. *Glob Change Biol* 6:196–210
- Hobbie SE, Miley TA, Weiss MS (2002) Carbon and nitrogen cycling in soils from different glacial surfaces in northern Alaska. *Ecosystems* 5:761–774
- Hobbie SE, Gough L, Shaver GR (2005) Species compositional differences on different-aged glacial landscapes drive contrasting responses of tundra to nutrient addition. *J Ecol* 93:770–782
- Hu FS, Higuera PE, Walsh JE, Chapman WL, Duffy PA, Brubaker LB, Chipman ML (2010) Tundra burning in Alaska: linkages to climatic change and sea ice retreat. *J Geophys Res* 115:G004002
- Hugelius G, Strauss J, Zubrzycki S, Harden JW, Schuur EAG, Ping C-L, Schirmermeister L, Grosse G, Michaelson GJ, Koven CD, O'Donnell JA, Elberling B, Mishra U, Camill P, Yu Z, Palmtag J, Kuhry P (2014) Estimated stocks of circumpolar permafrost carbon with quantified uncertainty ranges and identified data gaps. *Biogeosciences* 11:6573–6593
- Hyvönen R, Ågren GI (2001) Decomposer invasion rate, decomposer growth rate, and substrate chemical quality: how they influence soil organic matter turnover. *Can J For Res* 31:1594–1601
- Intergovernmental Panel on Climate Change (2007) Climate change 2007. In: Solomon S, Qin D, Manning M, Chen Z, Marquis M, Averyt KB, Tignor M, Miller HL (eds) the physical science basis. Contribution of working group I to the fourth assessment report of the intergovernmental panel on climate change. Cambridge University Press, Cambridge
- Jiang Y, Rastetter EB, Rocha AV, Pearce AR, Kwiatkowski BL, Shaver GR (2015) Modeling carbon–nutrient interactions during the early recovery of tundra after fire. *Ecol Appl* 25:1640–1652
- Jones BM, Kolden CA, Jandt R, Abatzoglou JT, Urban F, Arp CD (2009) Fire behavior, weather, and burn severity of the 2007 Anaktuvuk River Tundra Fire, North Slope, Alaska. *Arct Antarct Alp Res* 41:309–316
- Loladze I, Kuang Y, Elser JJ (2000) Stoichiometry in producer–grazer systems: linking energy flow with element cycling. *Bull Math Biol* 62:1137–1162
- Lorantny MM, Goetz SJ, Rastetter EB, Rocha AV, Shaver GR, Humphreys ER, Lafleur PM (2011) Scaling an instantaneous model of tundra NEE to the Arctic landscape. *Ecosystems* 14:76–93
- Mack MC, Schuur EAG, Bret-Harte MS, Shaver GR, Chapin FS III (2004) Ecosystem carbon storage in arctic tundra reduced by long-term nutrient fertilization. *Nature* 431:440–443
- Mack MC, Bret-Harte MS, Hollingsworth TN, Jandt RR, Schuur EAG, Shaver GR, Verbyla DL (2011) Carbon loss from an unprecedented Arctic tundra wildfire. *Nature* 475:489–492
- McGuire AD, Christensen TR, Hayes D, Heroult A, Euskirchen E, Yi Y, Kimball JS, Koven C, Lafleur P, Miller PA, Oechel W, Peylin P, Williams M (2012) An assessment of the carbon balance of arctic tundra: comparisons among observations, process models, and atmospheric inversions. *Biogeosci Discuss* 9:4543–4594
- McKane RB, Rastetter EB, Shaver GR, Nadelhoffer KJ, Giblin AE, Laundre JA, Chapin FS III (1997) Reconstruction and analysis of historical changes in carbon storage in arctic tundra. *Ecology* 78:1188–1198
- Melillo JM, Aber JD, Linkins AE, Ricca A, Fry B, Nadelhoffer KJ (1989) Carbon and nitrogen dynamics along the decay continuum: plant litter to soil organic matter. *Plant Soil* 115:189–198
- Mishra U, Riley WJ (2012) Alaskan soil carbon stocks: spatial variability and dependence on environmental factors. *Biogeosciences* 9:3637–3645
- Myers-Smith IH, Forbes BC, Wilmking M, Hallinger M, Lantz T, Blok D, Hik DS (2011) Shrub expansion in tundra ecosystems: dynamics, impacts and research priorities. *Environ Res Lett* 6:045509
- Nadelhoffer KJ, Giblin AE, Shaver GR, Laundre JA (1991) Effects of temperature and substrate quality on element mineralization in 6 Arctic soils. *Ecology* 72:242–253

- Oechel WC, Vourlitis GL, Hastings SJ, Zulueta RC, Hinzman L, Kane D (2000) Acclimation of ecosystem CO₂ exchange in the Alaskan Arctic in response to decadal climate warming. *Nature* 406:978–981
- Pearce AR, Rastetter EB, Kwiatkowski BL, Bowden WB, Mack MC, Jiang Y (2015) Recovery of arctic tundra from thermal erosion disturbance is constrained by nutrient accumulation: a modeling analysis. *Ecol Appl* 25(5):1271–1289
- Rastetter EB (2011) Modeling coupled biogeochemical cycles. *Front Ecol Environ* 9:68–73
- Rastetter EB, McKane RB, Shaver GR, Melillo JM (1992) Changes in C storage by terrestrial ecosystems: How C–N interactions restrict responses to CO₂ and temperature. *Water Air Soil Pollut* 64:327–344
- Rastetter EB, Ågren GI, Shaver GR (1997) Responses of N-limited ecosystems to increased CO₂: a balanced-nutrition, coupled-element-cycles model. *Ecol Appl* 7:444–460
- Rastetter EB, Yanai RD, Thomas RQ, Vadeboncoeur MA, Fahey TJ, Fisk MC, Kwiatkowski BL, Hamburg SP (2013) Recovery from disturbance requires resynchronization of ecosystem nutrient cycles. *Ecol Appl* 23:621–642
- Raynolds MK, Walker DA, Maier HA (2006) Alaska Arctic Tundra Vegetation Map. 1:4,000,000. U.S. Fish and Wildlife Service, Anchorage, AK
- Rocha AV, Loranty MM, Higuera PE, Mack MC, Hu FS, Jones BM, Breen AL, Rastetter EB, Goetz SJ, Shaver GR (2012) The footprint of Alaskan tundra fires during the past half-century: implications for surface properties and radiative forcing. *Environ Res Lett* 7. doi:10.1088/1748-9326/7/4/044039
- Rustad LE, Campbell J, Marion G, Norby R, Mitchell M, Hartley A, Gurevitch J (2001) A meta-analysis of the response of soil respiration, net nitrogen mineralization, and aboveground plant growth to experimental ecosystem warming. *Oecologia* 126:543–562
- Scenarios Network for Alaska planning (2013) <http://www.snap.uaf.edu>. Accessed 5 July 2012
- Schuur EAG, Crummer KG, Vogel JG, Mack MC (2007) Plant species composition and productivity following permafrost thaw and thermokarst in Alaskan tundra. *Ecosystems* 10:280–292
- Shaver GR, Chapin FS III (1980) Response to fertilization by various plant growth forms in an Alaskan tundra: nutrient accumulation and growth. *Ecology* 61(3):662–675
- Shaver GR, Chapin FS III (1991) Production: biomass relationships and elemental cycling in contrasting arctic vegetation types. *Ecol Monogr* 61:1–31
- Shaver GR, Jonasson S (1999) Response of arctic ecosystems to climate change: Results of long-term field experiments in Sweden and Alaska. *Polar Biol* 18:245–252
- Shaver GR, Jonasson S (2001) Productivity of Arctic Ecosystems. In: Mooney H, Roy J, Saugier B (eds) *Terrestrial global productivity*. Academic Press, New York, pp 189–210
- Shaver GR, Laundre JA (2006) Bulk precipitation collected during summer months on a per rain event basis at Toolik Field Station, North Slope of Alaska, Arctic LTER 1988–2007. <http://dx.doi.org/10.6073/pasta/cb6e3030fb69d2bf9549d8fe529a67fd>
- Shaver GR, Billings WD, Chapin FS III, Giblin AE, Nadelhoffer KJ, Oechel WC, Rastetter EB (1992) Global change and the carbon balance of arctic ecosystems. *Bioscience* 42:433–441
- Shaver GR, Bret-Harte SM, Jones MH, Johnstone J, Gough L, Laundre J, III Chapin FS (2001) Species composition interacts with fertilizer to control long-term change in tundra productivity. *Ecology* 82:3163–3181
- Shaver GR, Giblin AE, Nadelhoffer KJ, Thielert KK, Downs MR, Laundre JA, Rastetter EB (2006) Carbon turnover in Alaskan tundra soils: effects of organic matter quality, temperature, moisture and fertilizer. *J Ecol* 94:740–753
- Shaver GR, Street LE, Rastetter EB, van Wijk MT, Williams M (2007) Functional convergence in regulation of net CO₂ flux in heterogeneous tundra landscapes in Alaska and Sweden. *J Ecol* 95:802–817
- Sistla SA, Moore JC, Simpson RT, Gough L, Shaver GR, Schimel JP (2013) Long-term warming restructures Arctic tundra without changing net soil carbon storage. *Nature* 497:615–618
- Sitch S, McGuire AD, Kimball J, Gedney N, Gamon J, Engstrom R, McDonald KC (2007) Assessing the carbon balance of circumpolar Arctic tundra using remote sensing and process modelling. *Ecol Appl* 17:213–234
- Stow DA, Hope A, McGuire D, Verbyla D, Gamon J, Huemmrich F, Houston S, Racine C, Sturm M, Tape K, Hinzman L, Yoshikawa K, Tweedie C, Noyle B, Silapaswan C, Douglas D, Griffith B, Jia G, Epstein H, Walker D, Daeschner S, Petersen A, Zhou LM, Myneni R (2004) Remote sensing of vegetation and land-cover change in Arctic tundra ecosystems. *Remote Sens Environ* 89:281–308
- Street LE, Shaver GR, Williams M, van Wijk MT (2007) What is the relationship between changes in canopy leaf area and changes in photosynthetic CO₂ flux in arctic ecosystems? *J Ecol* 95:139–150
- Street LE, Shaver GR, Rastetter EB, van Wijk MT, Kaye BA, Williams M (2012) Incident radiation and the allocation of nitrogen within arctic plant canopies: implications for predicting gross primary productivity. *Glob Chang Biol* 18:2838–2852
- Verbyla D (2008) The greening and browning of Alaska based on 1982–2003 satellite data. *Glob Ecol Biogeogr* 17:547–555
- Walker DA, Epstein HE, Jia GJ, Balsler A, Copass C, Edwards EJ, Raynolds MK (2003) Phytomass, LAI, and NDVI in northern Alaska: Relationships to summer warmth, soil pH, plant functional types, and extrapolation to the circumpolar Arctic. *J Geophys Res* 108(D2):8169. doi:10.1029/2001JD000986
- Walker MD, Wahren CH, Hollister RD, Henry GHR, Ahlquist LE, Alatalo JM, Bret-Harte MS, Calef MP, Callaghan TV, Carroll AB, Epstein HE, Jonsdottir IS, Klein JA, Magnusson B, Molau U, Oberbauer SF, Rewa SP, Robinson CH, Shaver GR, Suding KN, Thompson CC, Tolvanen A, Totland Ø, Turner PL, Tweedie CE, Webber PJ, Wookey PA (2006) Plant community responses to experimental warming across the tundra biome. *Proc Natl Acad Sci* 103:1342–1346
- Weatherley LR, Miladinovic ND (2004) Comparison of the ion exchange uptake of ammonium ion onto New Zealand clinoptilolite and mordenite. *Water Res* 38:4305–4312
- Wilcox S (2012) National solar radiation database 1991–2010 update: user’s manual, Tech. Report NREL/TP-5500-

54824, Golden, CO, USA. <http://www.nrel.gov/docs/fy12osti/54824.pdf>

Yano Y, Shaver GR, Giblin AE, Rastetter EB, Nadelhoffer KJ (2010) Nitrogen dynamics in a small arctic watershed: retention and downhill movement of ^{15}N . *Ecol Monogr* 80:331–351

Zhang K, Kimball JS, Hogg EH, Zhao MS, Oechel WC, Cassano JJ, Running SW (2008) Satellite-based model detection of recent climate-driven changes in northern high-latitude vegetation productivity. *J Geophys Res* 113:G03033